

Vibrational Structure of Monosubstituted Octahydrosilasesquioxanes

Claudia Marcolli and Gion Calzaferri*

Department of Chemistry and Biochemistry, University of Berne, Freiestrasse 3, 3000 Berne 9, Switzerland

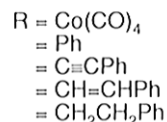
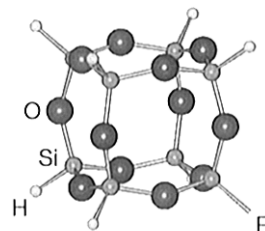
Received: February 28, 1997[⊗]

The IR and Raman spectra of the monosubstituted hydrosilasesquioxanes $\text{RH}_7\text{Si}_8\text{O}_{12}$, $\text{R} = \text{Co}(\text{CO})_4$, Ph , $\text{CH}=\text{CHPh}$, and $\text{CH}_2\text{CH}_2\text{Ph}$, have been analyzed by spectral correlation and a normal coordinate analysis. They were treated as a superposition of the spectra of the siloxane cage and the substituent. The molecules $\text{PhH}_7\text{Si}_8\text{O}_{12}$, $(\text{PhCH}=\text{CH})\text{H}_7\text{Si}_8\text{O}_{12}$, and $(\text{PhCH}_2\text{CH}_2)\text{H}_7\text{Si}_8\text{O}_{12}$ have allowed the investigation of the organic-substituted siloxane cage $\text{CH}_7\text{Si}_8\text{O}_{12}$, contributing each a case of an $\text{Si}-\text{C}_{\text{phenyl}}$, $\text{Si}-\text{C}_{\text{vinyl}}$, and $\text{Si}-\text{C}_{\text{alkyl}}$ bond, respectively. The force constants of the different $\text{Si}-\text{C}$ bonds were related to the $\text{Si}-\text{C}$ bond orders and extrapolated for $\text{Si}-\text{C}_{\text{acetyl}}$ of $(\text{PhC}\equiv\text{CH})\text{H}_7\text{Si}_8\text{O}_{12}$, which is not yet available. The inorganic-substituted hydrosilasesquioxane $[\text{Co}(\text{CO})_4(\text{H}_7\text{Si}_8\text{O}_{12})]$ could be analyzed the same way as the organic-substituted compounds and showed a similar pattern for the siloxane cage vibrations. Although most spectral features of the siloxane cages could be understood assuming a local C_{3v} symmetry, vibrations indicating a lower symmetry occurred in all monosubstituted compounds and could be attributed to vibrational coupling with modes of the substituent. Especially the totally symmetric ring-opening vibration at 456 cm^{-1} in $\text{H}_8\text{Si}_8\text{O}_{12}$ showed a specific dependence on the different substituents.

Introduction

Octasilasesquioxanes are members of the cage-shaped oligosilasesquioxanes of the general formula $(\text{RSiO}_{3/2})_{2n}$ ($n = 2, 3, 4, \dots$).¹ They show a cube-shaped Si_8O_{12} unit as illustrated in Scheme 1. During the past few years an increasing number of organo- or organometallo-functionalized silasesquioxanes have become available. They are discussed as oligomeric supramolecular materials,^{2,3} as sources for new organosiliceous polymers,^{4,5} and as precursors to organolithic macromolecular materials (OMM's)^{6–8} or hybrid inorganic–organic materials.^{9–11} Moreover, it has been shown that atomic hydrogen can be encapsulated stably in the Si_8O_{12} cage.¹² Hydrosilasesquioxanes ($\text{R} = \text{H}$) have been fruitfully viewed as readily available model compounds for studying specific aspects of zeolites or silica surfaces.^{13–18} Especially $\text{H}_8\text{Si}_8\text{O}_{12}$ has been thoroughly investigated by X-ray and neutron diffraction,^{19,20} as well as NMR²¹ and vibrational spectroscopies.^{14,22} Hydrosilation of $\text{H}_8\text{Si}_8\text{O}_{12}$ leads to monosubstituted and higher substituted octanuclear silasesquioxanes,^{23–25} which can be separated by size exclusion liquid chromatography.²⁶ The compounds $\text{RH}_7\text{Si}_8\text{O}_{12}$ with $\text{R} = \text{Co}(\text{CO})_4$, $\text{CH}=\text{CHPh}$, and $\text{CH}_2\text{CH}_2\text{Ph}$ illustrated in Scheme 1 have been synthesized by this method.^{27,28} $\text{PhH}_7\text{Si}_8\text{O}_{12}$ in contrast was obtained starting from a mixture of HSiCl_3 and PhSiCl_3 ,²⁹ $(\text{PhCH}_2\text{CH}_2)\text{H}_7\text{Si}_8\text{O}_{12}$, $\text{PhH}_7\text{Si}_8\text{O}_{12}$, and $(\text{PhCH}=\text{CH})\text{H}_7\text{Si}_8\text{O}_{12}$ form a series of molecules composed of a siloxane cage, which is connected to a phenyl group by a $\text{Si}-\text{C}_{\text{alkyl}}$, $\text{Si}-\text{C}_{\text{phenyl}}$, and $\text{Si}-\text{C}_{\text{vinyl}}$ bond, respectively. $(\text{PhC}\equiv\text{CH})\text{H}_7\text{Si}_8\text{O}_{12}$, which is not available yet, would complete this series by contributing the case of the $\text{Si}-\text{C}_{\text{acetyl}}$ bond. We are interested in the vibrational structure of these molecules for theoretical and practical reasons. The theoretical interest stems from their structural similarity with characteristic building elements of zeolites. This has allowed transfer of force constants determined for $\text{H}_8\text{Si}_8\text{O}_{12}$ to these extended structures.¹⁴ The notion of ring-opening vibrations, which was introduced for $O_h\text{-H}_8\text{Si}_8\text{O}_{12}$, opened a gate for studying the pore-opening vibrations, which are believed to play an important role in the dynamics and the

SCHEME 1: Investigated Monosubstituted Octahydrosilasesquioxanes $\text{RH}_7\text{Si}_8\text{O}_{12}$



transport properties of zeolites.¹⁵ $\text{H}_8\text{Si}_8\text{O}_{12}$, $\text{D}_8\text{Si}_8\text{O}_{12}$, and $\text{H}_{10}\text{-Si}_{10}\text{O}_{15}$ have therefore been thoroughly investigated by IR, Raman, and INS (inelastic neutron scattering) spectroscopies.²² Moreover, IR and Raman spectroscopies provide an important tool for the identification and characterization of silasesquioxanes. The vibrational structure of $\text{PhH}_7\text{Si}_8\text{O}_{12}$ has been discussed in detail on the basis of a normal coordinate analysis.²⁹ For $(\text{PhCH}=\text{CH})\text{H}_7\text{Si}_8\text{O}_{12}$ and $(\text{PhCH}_2\text{CH}_2)\text{H}_7\text{Si}_8\text{O}_{12}$ a preliminary analysis has been given in ref 30. It was shown that the IR and Raman spectra of the investigated compounds are best understood as superpositions of the spectra of the siloxane cages and the substituents.

In this work the analysis of monosubstituted hydrosilasesquioxanes will be extended to an inorganic-substituted octahydrosilasesquioxane. In $[\text{Co}(\text{CO})_4(\text{H}_7\text{Si}_8\text{O}_{12})]$ the $\text{Co}(\text{CO})_4$ substituent is connected to the siloxane cage by a $\text{Si}-\text{Co}$ bond. The IR and Raman spectra of this molecule will be treated the same way as the ones of the organic-substituted compounds. The investigated $\text{RH}_7\text{Si}_8\text{O}_{12}$ molecules, $\text{R} = \text{Co}(\text{CO})_4$, Ph , $\text{CH}=\text{CHPh}$, and $\text{CH}_2\text{CH}_2\text{Ph}$, form a good basis for a comparison of the vibrations of the substituted and unsubstituted siloxane cages. Special attention will be paid to the ring-opening vibrations. Moreover, the organic-substituted molecules allow a comparison of the $\text{Si}-\text{C}_{\text{alkyl}}$, $\text{Si}-\text{C}_{\text{vinyl}}$, and $\text{Si}-\text{C}_{\text{phenyl}}$ bonds.

* To whom correspondence should be addressed.

[⊗] Abstract published in *Advance ACS Abstracts*, June 1, 1997.

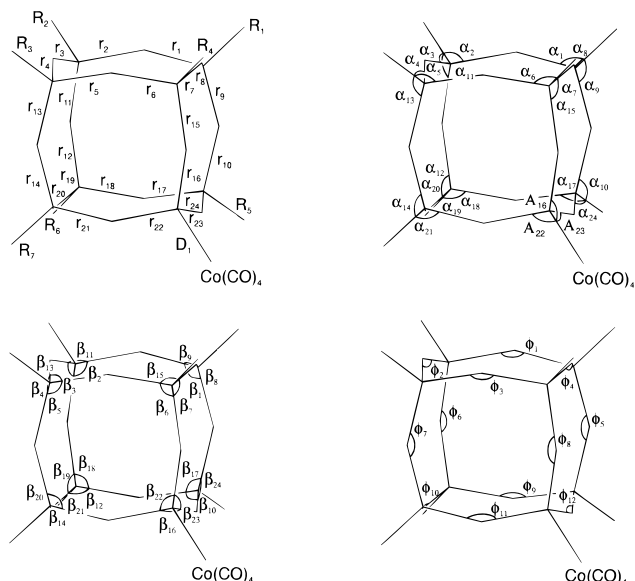


Figure 1. Numbering of the internal coordinates of the siloxane cage $H_7Si_8O_{12}$.

TABLE 1: Bond Lengths (Å) and Bond Angles (deg) for $[Co(CO)_4(H_7Si_8O_{12})]$

internal coordinates	values	internal coordinates	values
$R(Si-H)$	1.48	$T(Co-C_{ax})$	1.809
$r(Si-O)$	1.62	$S(Co-C_{eq})$	1.788
$\alpha(O-Si-H)$	109.5	$t(C_{ax}-O)$	1.128
$\beta(O-Si-H)$	109.5	$s(C_{eq}-O)$	1.131
$\phi(Si-O-Si)$	148.4	$\omega(Si-Co-C_{eq})$	83.9
$D(Si-Co)$	2.285	$\epsilon(C_{eq}-Co-C_{ax})$	96.1

The Si-C frequencies and force constants shall be related to the bond orders as determined by an EHMO calculation and extrapolated for Si-C_{acetyl}.

Experimental Section

Synthesis. The synthesis and purification of the investigated monosubstituted octahydrosilasesquioxanes are described in refs 23 and 27–30.

Spectroscopy. The IR transmission spectra were measured with a BOMEM DA3.01 FTIR spectrometer equipped with a liquid nitrogen-cooled MCT detector ($500-5000\text{ cm}^{-1}$), a liquid helium-cooled CuGe detector ($350-4000\text{ cm}^{-1}$), and a DTGS detector ($10-670\text{ cm}^{-1}$). A KBr beam splitter was applied for measurements above $\sim 650\text{ cm}^{-1}$ whereas in the range 350 to $\sim 700\text{ cm}^{-1}$ a $3\text{ }\mu\text{m}$ Mylar beam splitter was used. The spectrum of $(PhCH_2CH_2)H_7Si_8O_{12}$ was measured in CCl_4 and pentane ($960-650\text{ cm}^{-1}$) with the MCT (above 960 cm^{-1}) and the CuGe detectors and a resolution of 0.5 cm^{-1} . $(PhCH=CH)H_7Si_8O_{12}$ was measured in CCl_4 and heptane ($930-670\text{ cm}^{-1}$) with the MCT detector (above 670 cm^{-1} , resolution = 0.5 cm^{-1}) and the DTGS detector (resolution = 2 cm^{-1}). $[Co(CO)_4(H_7Si_8O_{12})]$ was measured in CCl_4 with the MCT (above 824 cm^{-1} , resolution = 1 cm^{-1}) and the DTGS detector (below 650 cm^{-1} , resolution = 2 cm^{-1}). Between 824 and 650 cm^{-1} the spectrum was interpolated. The detailed measuring conditions for $(C_6H_{13})H_7Si_8O_{12}$ are found in ref 28 and for $PhH_7Si_8O_{12}$ in ref 29.

Fourier-transform Raman spectra were recorded with the Bomem Raman accessory of the same spectrometer. The interferometer was equipped with a quartz beam splitter and a liquid nitrogen-cooled InGaAs detector. The continuous-wave Nd³⁺:YAG laser (Quatronix Model 114) was run in the

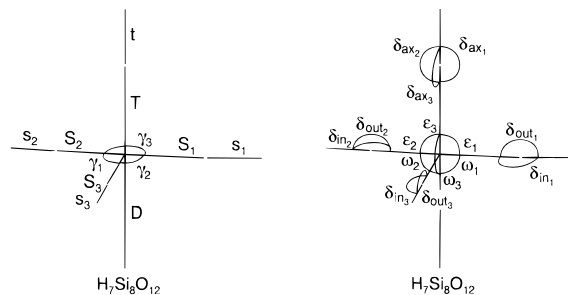


Figure 2. Numbering of the internal coordinates of the carbonyl group $Co(CO)_4$.

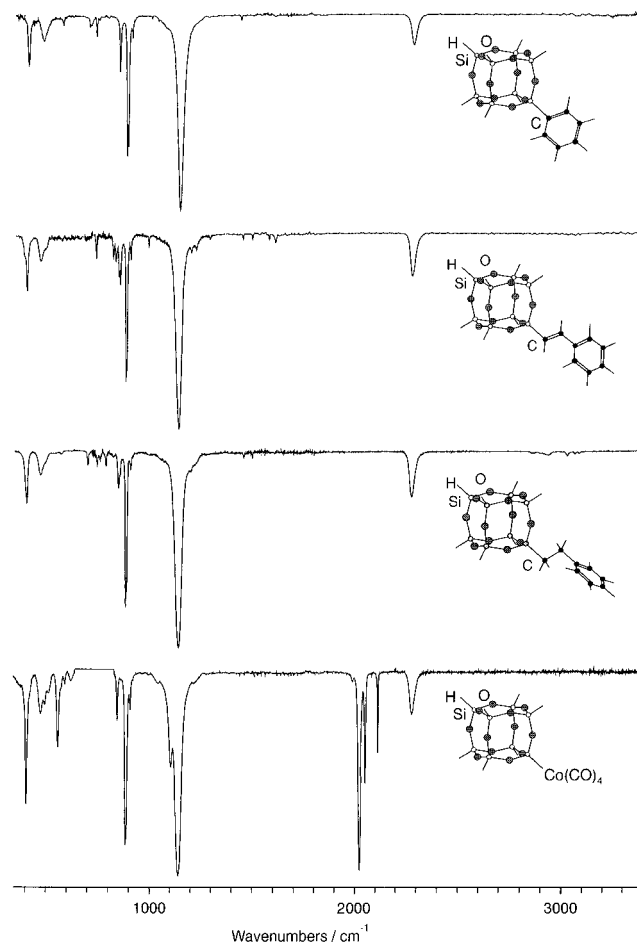


Figure 3. Transmission IR spectra of the investigated monosubstituted octahydrosilasesquioxanes $RH_7Si_8O_{12}$.

transverse electromagnetic mode TEM_{00} at 9395 cm^{-1} . Rayleigh scattering was blocked by three holographic super notch filters (Kaiser Optical Systems) in a 6° angle position. A 2 mm thick anodized aluminum plate with a 1 mm diameter hole into which the probe was slightly pressed served as sample holder. As the spectrum of $[Co(CO)_4(H_7Si_8O_{12})]$ was not corrected for filter characteristics, the intensities of the two peaks close to the detection limit at 115 and 109 cm^{-1} are lowered by the filter characteristics.

Calculations. The vibrational analysis was performed by the Wilson GF matrix method³¹ with the computer program package QCMP0676.³² The force field of $[Co(CO)_4(H_7Si_8O_{12})]$ is based on a force field determined on IR and FT-Raman data of $H_8Si_8O_{12}$ and $D_8Si_8O_{12}$ for the siloxane cage¹⁴ and on one developed by van den Berg and Oskam for $[Co(CO)_4(MX_3)]$ compounds ($M = Si, Ge, Sn; X = H, D, F, Cl, Br, I$)³³ for the $Co(CO)_4$ group. The bond lengths and angles are listed in Table 1. They correspond for the siloxane cage to the ones used for

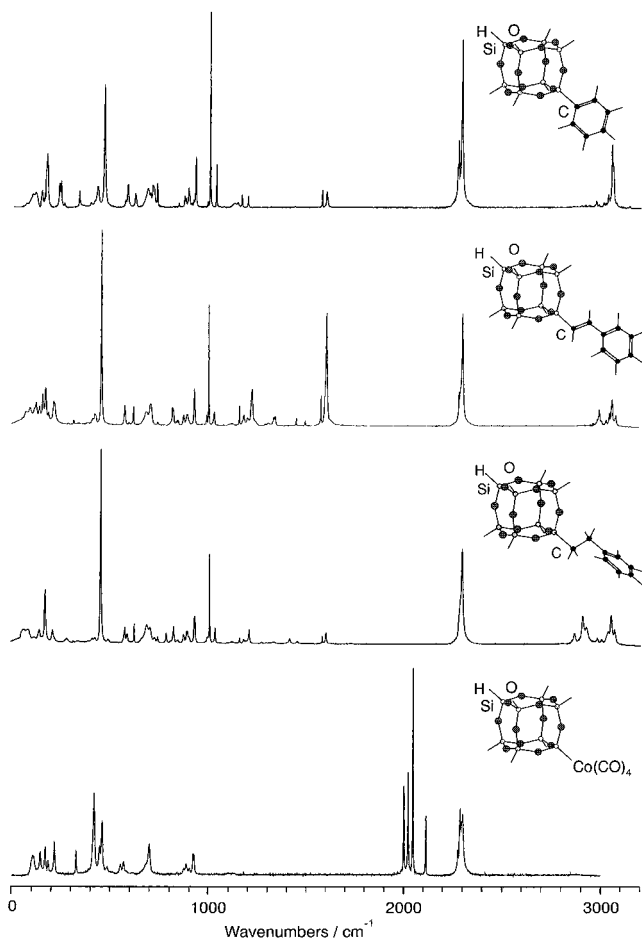


Figure 4. FT-Raman spectra of the investigated monosubstituted octahydrosilasesquioxanes $\text{RH}_7\text{Si}_8\text{O}_{12}$.

$\text{H}_8\text{Si}_8\text{O}_{12}$ and for $\text{Co}(\text{CO})_4$ to average values from the X-ray diffraction analysis of $[\text{Co}(\text{CO})_4(\text{H}_7\text{Si}_8\text{O}_{12})]$. The numbering of the internal coordinates is shown in Figures 1 and 2. The torsion $\tau_{\text{Si}-\text{Co}}$ between the $\text{Co}(\text{CO})_4$ group and the siloxane cage was not included into the calculation, because it is expected below the detection limit and has hardly any influence on other vibrations. A description of the force fields of the other investigated molecules can be found in ref 34. Molecular orbital calculations have been carried out with the modified QCPE116³⁵ program; see ref 36.

Results and Discussion

Figures 3 and 4 show the IR and Raman spectra of the four investigated monosubstituted octahydrosilasesquioxanes. It was shown that the spectra of $\text{RH}_7\text{Si}_8\text{O}_{12}$ ($\text{R} = \text{Ph}, \text{CH}=\text{CHPh}, \text{CH}_2\text{-CH}_2\text{Ph}$) can be understood as superpositions of the vibrational structure of the substituent and the siloxane cage.^{29,30} Although complex spectra are expected because of the size and low symmetry of these molecules, most peaks can be assigned by spectral correlations with similar compounds. Yet, for a final assignment a normal coordinate analysis of all fundamentals was found to be necessary. The symmetry reduction was best described by treating the substituent as a point mass. This led to local C_{3v} symmetry for the siloxane cages. Peaks or splittings, which cannot be explained by this local symmetry, also occurred and were due to vibrational coupling with modes of the substituent.

Vibrational Analysis of $[\text{Co}(\text{CO})_4(\text{H}_7\text{Si}_8\text{O}_{12})]$

IR and Raman Spectra. This molecule has an ideal symmetry of C_{3v} . X-ray diffraction has shown deviations for

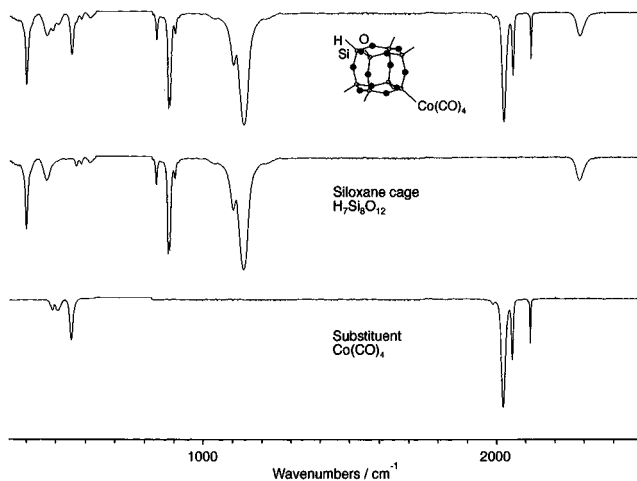


Figure 5. Transmission IR spectrum of $[\text{Co}(\text{CO})_4(\text{H}_7\text{Si}_8\text{O}_{12})]$ divided into the lines due to the siloxane cage and the substituent.

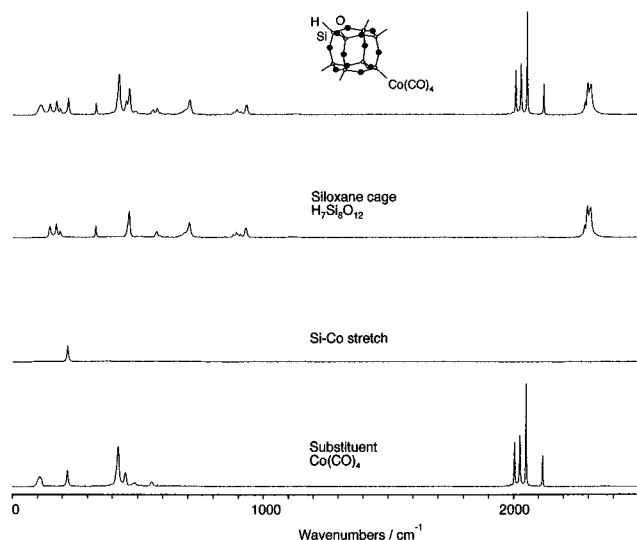


Figure 6. Fourier-transform Raman spectrum of $[\text{Co}(\text{CO})_4(\text{H}_7\text{Si}_8\text{O}_{12})]$ divided into the lines due to the siloxane cage, the substituent, and the Si-Co stretch.

both the siloxane cage and the $\text{Co}(\text{CO})_4$ group. The $\text{H}_7\text{Si}_8\text{O}_{12}$ fragment exhibits distortions around, and originating from, the Si atom to which the $\text{Co}(\text{CO})_4$ fragment binds.²⁷

Figures 5 and 6 show the IR and Raman spectra divided into the contributions of the siloxane cage, the $\text{Co}(\text{CO})_4$ group, and the Si-Co bond. This division was achieved by spectral correlations with $[\text{Co}(\text{CO})_4(\text{SiX}_3)]$ compounds ($\text{X} = \text{H}, \text{F}, \text{Cl}$)^{33,37,38} and the normal coordinate analysis of the molecule. It can be seen that the $\text{Co}(\text{CO})_4$ fragment gives rise to very intense peaks. In the Raman spectrum of $[\text{Co}(\text{CO})_4(\text{H}_7\text{Si}_8\text{O}_{12})]$ they form the strongest lines, and in the IR spectrum they are of the same order of magnitude as the siloxane cage bands, which are also known to be responsible for very intense absorptions.

Above 800 cm^{-1} the spectra can be divided according to group frequencies into the following frequency regions: $\delta(\text{O}-\text{Si}-\text{H})$, $850-950 \text{ cm}^{-1}$; $\nu_{\text{asym}}(\text{Si}-\text{O}-\text{Si})$, $1100-1200 \text{ cm}^{-1}$; $\nu(\text{C}-\text{O})$, $2000-2150 \text{ cm}^{-1}$; $\nu(\text{Si}-\text{H})$, $>2200 \text{ cm}^{-1}$. As these regions do not overlap, an assignment to either siloxane cage or $\text{Co}(\text{CO})_4$ group vibrations is straightforward. Below 800 cm^{-1} the symmetrical Si-O-Si stretching ($750-550 \text{ cm}^{-1}$), the O-Si-O bending ($500-150 \text{ cm}^{-1}$), and the Si-O-Si bending vibrations ($<100 \text{ cm}^{-1}$) of the siloxane cage as well as the CoC stretching and CoCO deformation modes ($650-$

TABLE 2: Definition of the Simplified General Valence Force Field for [Co(CO)₄(H₇Si₈O₁₂)]

	R_1	r_1	r_2	r_8	α_1	α_8	β_1	β_8	ϕ	D	A	S_1	S_2	T	s_1	s_2	t	ω_1	ϵ_1	γ_1	δ_{out1}	δ_{out2}	δ_{in1}	δ_{ax1}	
R_1	f_R																								
r_1	0	f_r																							
r_2	0	f_{rr}	f_r																						
r_8	0	f_{rr}	0	f_r																					
α_1	0	$f_{r\alpha}$	0	$f_{r\alpha}$	$f_{\alpha\alpha}$																				
α_8	0	$f_{r\alpha}$	0	$f_{r\alpha}$	$f_{\alpha\alpha}$	$f_{\alpha\alpha}$																			
β_1	0	$f_{r\beta}$	0	$f_{r\beta}$	$f_{\alpha\beta}$	$f_{\alpha\beta}$	$f_{\beta\beta}$																		
β_8	0	$f_{r\beta}$	0	$f_{r\beta}$	$f_{\alpha\beta}$	$f_{\alpha\beta}$	$f_{\beta\beta}$	$f_{\beta\beta}$																	
ϕ	0	$f_{r\phi}$	$f_{r\phi}$	0	$f_{\alpha\phi}$	0	$f_{\beta\phi}$	0	f_{ϕ}																
D	0	0	0	0	0	0	0	0	0	F_D															
A	0	0	0	0	0	0	0	0	0	F_{AD}	F_A														
S_1										0	0	F_S													
S_2										0	0	F_{SS}	F_S												
T										0	0	F_{ST}	F_{ST}	F_T											
s_1										0	0	F_{sS}	F'_{sS}	0	F_s										
s_2										0	0	F'_{sS}	F_{sS}	0	F_{ss}	F_s									
t										0	0	0	0	F_{tT}	F_{st}	F_{st}	F_t								
ω_1										0	0	0	0	0	0	0	0	F_ω							
ϵ_1										0	0	0	0	0	0	0	0	0	F_ϵ						
γ_1										0	0	0	0	0	0	0	0	0	0	F_γ					
δ_{out1}										0	0	0	0	$F_{T\delta_{out}}$	0	0	0	0	0	0	$F_{\delta_{out}}$				
δ_{out2}										0	0	0	0	$F_{T\delta_{out}}$	0	0	0	0	0	0	$F_{\delta_{out}}$	$F_{\delta_{out}}$			
δ_{in1}										0	0	0	0	0	0	0	0	0	0	0	0	0	$F_{\delta_{in}}$		
δ_{ax1}										0	0	0	$F_{S\delta_{ax}}$	0	0	0	0	0	0	0	0	0	0	$F_{\delta_{ax}}$	

TABLE 3: Internal Force Constants for [Co(CO)₄(H₇Si₈O₁₂)]

force const ^a	values	force const ^a	values	force const ^a	values
H ₇ Si ₈ O ₁₂					
f_R	2.96	f_{rr}	0.153	$f_{\alpha\alpha}$	0
f_r	5.10	$f_{r\alpha}$	0.188	$f_{\beta\beta}$	0
f_{α}	0.601	$f_{r\alpha}$	0	$f_{\alpha\beta}$	-0.095
f_{β}	0.895	$f_{r\beta}$	-0.016	$f'_{\alpha\beta}$	-0.175
f_{ϕ}	0.091	$f_{r\beta}$	0.144	$f_{\alpha\phi}$	0.019
f_{rr}	0.275	$f_{r\phi}$	0.036	$f_{\beta\phi}$	0.0026
Co(CO) ₄					
F_D	1.73	F_γ	0.49	F'_{sS}	0.11
F_A	0.57	$F_{\delta_{out}}$	0.68	F_{ss}	0.37
F_S	2.41	$F_{\delta_{in}}$	0.29	F_{tT}	0.55
F_T	2.25	$F_{\delta_{ax}}$	0.39	F_{st}	0.27
F_s	16.64	F_{AD}	0.25	$F_{T\delta_{out}}$	-0.08
F_t	17.33	F_{SS}	0.26	$F_{\delta\delta_{out}}$	-0.03
F_ω	0.38	F_{ST}	0.13	$F_{S\delta_{ax}}$	0.12
F_ϵ	0.51	F_{sS}	0.55		

^a Force constants units: stretching constants, mdyn/Å; bending constants, mdyn Å/rad²; stretch bend interactions, mdyn/rad.

300 cm⁻¹) of the Co(CO)₄ group occur. For a final assignment a normal coordinate analysis was therefore carried out.

Force Field. The modified general valence force field of [Co(CO)₄(H₇Si₈O₁₂)] is defined in Table 2, and the force constant values are given in Table 3. For the siloxane cage the same force constant definitions and values were used as for H₈-Si₈O₁₂. Additional force constants were introduced for the part involving the Si-Co bond. The definitions for the Co(CO)₄ group are based on the ones of ref 33. The values were determined by a fit to the IR and Raman frequencies of [Co(CO)₄(H₇Si₈O₁₂)] using the force constants of [Co(CO)₄(SiCl₃)] as starting values. The calculated frequencies are listed and compared with the experimental ones in Table 4. The assignment to symmetry types assuming an idealized C_{3v} symmetry and the correlation with the symmetry species of O_h-H₈Si₈O₁₂ is also given in this table.

Table 2 shows that it is possible to describe [Co(CO)₄(H₇-Si₈O₁₂)] with a relatively restricted number of interaction force constants. Particularly those between the three parts, siloxane cage, Si-Co bond, and Co(CO)₄ group, can be neglected. This confirms the notion of [Co(CO)₄(H₇Si₈O₁₂)] as being composed

of relatively independently vibrating moieties. The finally obtained force constants led to a good agreement of the calculated and measured frequencies as shown in Table 4. All peaks could be assigned to either vibrations of the substituent or the siloxane cage with one exception: the two vibrations at 461 and 449 cm⁻¹ in the Raman spectrum both show similar contributions of axial CoC stretching and O-Si-O bending movements.

CO Stretching Vibrations. The CO stretching vibrations, which are situated at ca. 2000 cm⁻¹, have been investigated thoroughly for different metal carbonyl compounds.³⁹⁻⁴² Assuming C_{3v} symmetry for the Co(CO)₄ fragment, they form an E and two A₁ type vibrations. The similar intensities of the two A₁ modes exhibited in the IR spectra of different metal carbonyl compounds led to the conclusion that the equatorial and the axial A₁ CO stretching movements are coupled. This was also confirmed by the depolarization ratio observed in the Raman spectra of [Co(CO)₄(SiCl₃)], [Co(CO)₄(GeCl₃)], and [Co(CO)₄(GeBr₃)] in solution.^{37,42} The vibration of [Co(CO)₄(H₇-Si₈O₁₂)] at 2111 (IR)/2110 cm⁻¹ (Raman) forms therefore the in-phase and the one at 2050 (IR)/2044 (Raman) cm⁻¹ the out-of-phase combination of the axial and equatorial CO stretching coordinates.

Si-Co Stretching Vibration. The Si-Co stretching vibration is assigned to the sharp Raman peak of medium intensity at 220 cm⁻¹, which exhibits 33% Si-Co stretching character in the potential energy distribution. The vibration at 329 cm⁻¹ also showed considerable Si-Co stretching character (15%). Si-Co stretching vibrations of similar compounds are located at 318 cm⁻¹ ([Co(CO)₄(SiH₃)]), 307 cm⁻¹ ([Co(CO)₄(SiCl₃)]), and 246 cm⁻¹ ([Co(CO)₄(SiF₃)]). The O-Si-Co bending vibration was below the detection limit.

The siloxane cage vibrations show a similar pattern as in other monosubstituted octahydrosilasesquioxanes and will therefore be discussed in the next section together with the siloxane cage spectra of the other investigated compounds.

Siloxane Cage Vibrations of Monosubstituted Octahydrosilasesquioxanes

A comparison of the siloxane cage vibrations of the RH₇-Si₈O₁₂ molecules (R = Co(CO)₄, Ph, CH=CHPh, CH₂CH₂Ph,

TABLE 4: Observed and Calculated Frequencies for [Co(CO)₄(H₇Si₈O₁₂)] (ν = Stretch, δ = Bending)

symmetry type		wavenumber/cm ⁻¹			vibration type
<i>O_h</i>	<i>C_{3v}</i>	IR	Raman	calc	
A _{1g}	A ₁		2297	2275	$\nu(\text{Si-H})$
T _{2g}	E, A ₁		2301/2292, 2285	2275, 2275	$\nu(\text{Si-H})$
T _{1u}	A ₁ , E	2276, 2276	2285, 2274	2275, 2275	$\nu(\text{Si-H})$
	A ₁	2111	2110	2111	$\nu(\text{CO})$
	A ₁	2050	2044	2046	$\nu(\text{CO})$
	E	2021	2020/1998	2020	$\nu(\text{CO})$
		1984			$\nu(^{13}\text{CO})$
T _{1g}	E, A ₂			1161, 1161	$\delta_{\text{asym}}(\text{Si-O-Si})$
E _u	E			1159	$\delta_{\text{asym}}(\text{Si-O-Si})$
T _{1u}	E, A ₁	1138, 1138		1143, 1143	$\delta_{\text{asym}}(\text{Si-O-Si})$
T _{2g}	A ₁ , E	1101	~1117, ~1117	1117, 1116	$\delta_{\text{asym}}(\text{Si-O-Si})$
A _{2u}	A ₁			1083	$\delta_{\text{asym}}(\text{Si-O-Si})$
E _g	E	916	928/923	921	$\delta(\text{O-Si-H})$
T _{2u}	A ₂ , E	-, 904	-, 904	918, 910	$\delta(\text{O-Si-H})$
T _{2g}	A ₁ , E	-, 886	893, 888	894, 889	$\delta(\text{O-Si-H})$
T _{1u}	A ₁ , E	886, 881	878, 875	882, 874	$\delta(\text{O-Si-H})$
T _{1g}	A ₂ , E	857, 840	-, 841	865, 864	$\delta(\text{O-Si-H})$
E _g	E		701	714	$\nu_{\text{sym}}(\text{Si-O-Si})$
T _{2u}	E, A ₂		684	687, 682	$\nu_{\text{sym}}(\text{Si-O-Si})$
T _{2g}	A ₁ , E	613	~616	625, 621	$\nu_{\text{sym}}(\text{Si-O-Si})$
T _{1u}	A ₁ , E	584, 565	585, -	586, 572	$\nu_{\text{sym}}(\text{O-Si-O})$
A _{1g}	A ₁		571	575	$\delta(\text{O-Si-O})$
	E	552	554	557	$\delta(\text{CoCO})_{\text{out}}$
	A ₁	552	554	553	$\delta(\text{CoCO})_{\text{out}}$
	E	507		504	$\nu(\text{CoC})_{\text{eq}} + \delta(\text{CoCO})_{\text{ax}}$
	E	488	487	490	$\delta(\text{CoCO})_{\text{ax}} + \nu(\text{CoC})_{\text{eq}}$
T _{1u}	E, A ₁	469, 469		487, 480	$\nu_{\text{sym}}(\text{O-Si-O})$
A _{1g}	A ₁		461	468	$\nu_{\text{sym}}(\text{O-Si-O}) + \nu(\text{CoC})_{\text{ax}}$
	A ₁		449	445	$\nu(\text{CoC})_{\text{ax}} + \nu_{\text{sym}}(\text{O-Si-O})$
T _{2g}	E, A ₁			426, 417	$\delta(\text{O-Si-O})$
E _g	E			422	$\delta(\text{O-Si-O})$
	A ₁		420	421	$\nu(\text{CoC})_{\text{eq}}$
T _{1u}	A ₁ , E	399, 399		402, 398	$\delta(\text{O-Si-O})$
	E		393	393	$\delta(\text{CoCO})_{\text{in}}$
T _{1g}	E, A ₂			360, 356	$\delta(\text{O-Si-O})$
	A ₂			331	$\delta(\text{CoCO})_{\text{in}}$
A _{2u}	A ₁		329	316	$\delta(\text{O-Si-O})$
T _{2u}	E, A ₂			305, 303	$\delta(\text{O-Si-O})$
A _{2u}	A ₁		220	219	$\nu(\text{Si-Co})$
E _u	E		190/187	183	$\delta(\text{O-Si-O})$
T _{2g}	E, A ₁		173, 147	168, 144	$\delta(\text{O-Si-O})$
	E		115	122	$\delta(\text{CCoC})$
	E		109	109	$\delta(\text{CCoC})$
E _u	E			100	$\delta(\text{Si-O-Si}) + \delta(\text{OSiCo})$
	A ₁			82	$\delta(\text{CCoC})$
E _g	E			77	$\delta(\text{Si-O-Si})$
T _{2u}	E, A ₂			70,68	$\delta(\text{Si-O-Si}) + \delta(\text{SiCoC})$
	E			30	$\delta(\text{SiCoC}) + \delta(\text{OSiCo})$

and C₆H₁₃ (only IR)), and H₈Si₈O₁₂ is given in Table 5 for the IR and in Table 6 for the Raman spectra. Compared with H₈-Si₈O₁₂ no large frequency shifts are observed. It can be seen that the introduction of a substituent gives rise to additional peaks and peak splittings. The influence of the substituent will be discussed below in detail.

Si-H Stretching Vibrations (2200–2300 cm⁻¹). This region consists in the IR spectra of all monosubstituted compounds of one absorption, which exhibits a slight broadening due to the substituent (fwhh = 28–30 cm⁻¹ compared with 26 cm⁻¹ in H₈Si₈O₁₂).

In the Raman spectra the Si-H stretching region is less uniform. The number of peaks and shoulders varies from two for (PhCH₂CH₂)H₇Si₈O₁₂ to six for [Co(CO)₄(H₇Si₈O₁₂)]. The considered RH₇Si₈O₁₂ molecules show a shift of 5–11 cm⁻¹ to

lower energy for the totally symmetric peak (at 2302 cm⁻¹ in H₈Si₈O₁₂). The T_{2g} $\nu(\text{Si-H})$ of H₈Si₈O₁₂ exhibits in the Raman spectrum of the solid a splitting of 10 cm⁻¹ due to the symmetry reduction to S₆ in the crystal. In the case of an organic substituent this splitting is reduced. This is in accordance with the X-ray diffractions of (C₆H₁₃)H₇Si₈O₁₂, and PhH₇Si₈O₁₂, which indicate rather smaller distortions of the siloxane cage for these molecules than for H₈Si₈O₁₂. It cannot be decided whether the splittings in the monosubstituted compounds are due to interactions in the crystal or to the influence of the substituent. The Raman spectrum of [Co(CO)₄(H₇Si₈O₁₂)] is rather complex in this region, so that a definite assignment is difficult. The one given in Table 6 can be considered as the most probable. The Si-H stretching regions are, with the exception of the one of [Co(CO)₄(H₇Si₈O₁₂)], in accordance with a local C_{3v} symmetry for the siloxane cage.

Antisymmetrical Si-O-Si Stretching Vibrations (1100–1200 cm⁻¹). The IR spectrum of H₈Si₈O₁₂ consists in this region of one intense broad band. The full width at half-height increases from 27 cm⁻¹ in H₈Si₈O₁₂ to 33–38 cm⁻¹ in the monosubstituted molecules. As the only compound, [Co(CO)₄(H₇-Si₈O₁₂)] shows a shoulder at 1101 cm⁻¹ which can be correlated with the T_{2g} $\nu_{\text{asym}}(\text{Si-O-Si})$ stretching mode. The antisymmetrical Si-O-Si stretching vibrations appear as broad weak features in the Raman spectra of the monosubstituted molecules. Their maxima correlate well with the one of the Raman active T_{2g} $\nu_{\text{asym}}(\text{Si-O-Si})$ of H₈Si₈O₁₂. Only PhH₇Si₈O₁₂ shows two distinct peaks in this region. This is in accordance with the normal coordinate analysis, which predicts a splitting of the T_{2g} $\nu_{\text{asym}}(\text{Si-O-Si})$ in the case of R = Ph, due to mixing with vibrations of the phenyl substituent ($\nu(\text{C-C})$, $\delta(\text{C-H})$).

O-Si-H Bending Vibrations (800–950 cm⁻¹). This region shows a typical pattern for monosubstituted octahydrosilasesquioxanes. Assuming C_{3v} symmetry, nine modes are expected, seven IR- and Raman-active (2 A₁, 5 E) and two inactive ones (2 A₂). The intense doublet at ca. 885 cm⁻¹ in the IR spectra can be correlated with the IR-active T_{1u} and the Raman-active T_{2g} $\delta(\text{O-Si-H})$ of H₈Si₈O₁₂. The peak at ca. 850 cm⁻¹ correlates with the inactive T_{1g} $\delta(\text{O-Si-H})$ of H₈-Si₈O₁₂. It appears in several monosubstituted compounds as a doublet, which is not in agreement with a local C_{3v} symmetry.

The Raman spectra of the monosubstituted compounds show seven to eight features in this region, some of them corresponding to a lower symmetry than C_{3v}. Only PhH₇Si₈O₁₂ is fully compatible with a local C_{3v} symmetry.

Vibrations of the Framework between 800 and 500 cm⁻¹. This region consists for O_h-H₈Si₈O₁₂ of five modes: one is IR (T_{1u}), three are Raman (E_g, T_{2g}, A_{1g}), and one is inactive (T_{2u}). The IR spectra of the monosubstituted hydrosilasesquioxanes show rather weak absorptions with intensities that are dependent on the specific substituents. The Raman spectra exhibit in all investigated RH₇Si₈O₁₂ compounds three peaks. The A_{1g} $\delta(\text{O-Si-O})$ appears at 580 cm⁻¹ in H₈Si₈O₁₂ and shows small frequency shifts depending on the specific substituents. The inactive T_{2u} $\nu_{\text{sym}}(\text{Si-O-Si})$ forms in all monosubstituted compounds a band of medium intensity between 680 and 690 cm⁻¹. The E_g $\nu_{\text{sym}}(\text{Si-O-Si})$ at 697 cm⁻¹ in H₈Si₈O₁₂ shows splittings of different size depending on the substituent. These splittings were predicted by the normal coordinate analysis and are due to coupling effects. For RH₇Si₈O₁₂ (R = Ph, CH=CHPh, and CH₂CH₂Ph), the T_{2g} $\nu_{\text{sym}}(\text{Si-O-Si})$ at 610 cm⁻¹ in H₈-Si₈O₁₂ is hidden behind the $\delta(\text{C-C})$ mode at ca. 620 cm⁻¹ of the phenyl ring. For R = CH=CHPh this mode shows a larger splitting, and the A₁ component could be observed.

TABLE 5: IR Frequencies of the Siloxane Cage Vibrations of Different Monosubstituted Octahydrosilasesquioxanes, $\text{RH}_7\text{Si}_8\text{O}_{12}$, and the Unsubstituted Compound ($\text{R} = \text{H}$)

wavenumber/cm ⁻¹						symmetry		vibration type
R = Co(CO) ₄	R = Ph	R = CH=CHPh	R = CH ₂ CH ₂ Ph	R = C ₆ H ₁₃	R = H	C _{3v}	O _h	
2276, 2276	2274, 2274	2275, 2275	2274, 2274	2274	2277	A ₁ , E	T _{1u}	$\nu(\text{Si}-\text{H})$
1138, 1138	1140, 1140	1140, 1140	1141, 1141	1139	1141	A ₁ , E	T _{1u}	$\nu_{\text{asym}}(\text{Si}-\text{O}-\text{Si})$
1101						A ₁ , E	T _{2g}	$\nu_{\text{asym}}(\text{Si}-\text{O}-\text{Si})$
916	915	915	916	916		E	E _g	$\delta(\text{O}-\text{Si}-\text{H})$
-, 904	-, 905	-, 905	-, 905	-, 905		A ₂ , E	T _{2u}	$\delta(\text{O}-\text{Si}-\text{H})$
-, 886	-, 886	-, 886	-, 886	-, 887		A ₁ , E	T _{2g}	$\delta(\text{O}-\text{Si}-\text{H})$
886, 881	886, 881	886, 883	886, 882	887, 882	881	A ₁ , E	T _{1u}	$\delta(\text{O}-\text{Si}-\text{H})$
857, 840	-, 844	854, 848	852, 846	-, 846		A ₂ , E	T _{1g}	$\delta(\text{O}-\text{Si}-\text{H})$
	718/704					E	E _g	$\nu_{\text{sym}}(\text{Si}-\text{O}-\text{Si})$
613			607, 622/18			A ₁ , E	T _{2g}	$\nu_{\text{sym}}(\text{Si}-\text{O}-\text{Si})$
			573	572		A ₁	A _{1g}	$\delta(\text{O}-\text{Si}-\text{O})$
584, 565	-, 568		-, 568		566	A ₁ , E	T _{1u}	$\nu_{\text{sym}}(\text{O}-\text{Si}-\text{O})$
469, 469	475, 475	469, 469	468, 468	468	465	A ₁ , E	T _{1u}	$\nu_{\text{sym}}(\text{O}-\text{Si}-\text{O})$
399, 399	401, 401	402, 388	395, 402	401	399	A ₁ , E	T _{1u}	$\delta(\text{O}-\text{Si}-\text{O})$

TABLE 6: Raman Frequencies of the Siloxane Cage Vibrations of Different Monosubstituted Octahydrosilasesquioxanes $\text{RH}_7\text{Si}_8\text{O}_{12}$ and the Unsubstituted Compound ($\text{R} = \text{H}$)

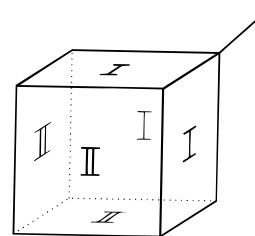
wavenumber/cm ⁻¹				symmetry		H ₈ Si ₈ O ₁₂	vibration type
R = Co(CO) ₄	R = Ph	R = CH=CHPh	R = CH ₂ CH ₂ Ph	C _{3v}	O _h		
2297	2291	2295	2295	A ₁ , E	A _{1g}	2302	$\nu(\text{Si}-\text{H})$
2285, 2301/2292	2278, 2285	2284, 2278	2286, 2286	A ₁ , E	T _{2g}	2296, 2286	$\nu(\text{Si}-\text{H})$
2285, 2274	2269, 2275			A ₁ , E	T _{1u}		$\nu(\text{Si}-\text{H})$
~1117, ~1117	1140, 1121	1119, 1119	1118, 1118	A ₁ , E	T _{2g}	1117	$\nu_{\text{asym}}(\text{Si}-\text{O}-\text{Si})$
928/923	925	927	928/26	E	E _g	932	$\delta(\text{O}-\text{Si}-\text{H})$
-, 904	-, 904	-, 900	-, 899	A ₂ , E	T _{2u}		$\delta(\text{O}-\text{Si}-\text{H})$
893, 888	893, 889	894, 890	890, 888	A ₁ , E	T _{2g}	897, 883	$\delta(\text{O}-\text{Si}-\text{H})$
878, 875	875, 868	874, 874	873, 871	A ₁ , E	T _{1u}		$\delta(\text{O}-\text{Si}-\text{H})$
-, 841	-, 839	847, 842	-, 840	A ₂ , E	T _{1g}		$\delta(\text{O}-\text{Si}-\text{H})$
701	712/707	706	726/703	E	E _g	697	$\nu_{\text{sym}}(\text{Si}-\text{O}-\text{Si})$
684	682, 682	688, 684/682	685	A ₂ , E	T _{2u}		$\nu_{\text{sym}}(\text{Si}-\text{O}-\text{Si})$
~616		597, -		A ₁ , E	T _{2g}	610	$\nu_{\text{sym}}(\text{Si}-\text{O}-\text{Si})$
571	580	575	575	A ₁	A _{1g}	580	$\delta(\text{O}-\text{Si}-\text{O})$
585, -	-, 569	532, 572		A ₁ , E	T _{1u}		$\nu_{\text{sym}}(\text{O}-\text{Si}-\text{O})$
461 (449)	462	455	452	A ₁	A _{1g}	456	$\nu_{\text{sym}}(\text{O}-\text{Si}-\text{O})$
	427	423/427	410, 423	A ₁ , E	T _{2g}	414	$\delta(\text{O}-\text{Si}-\text{O})$
	412	411	410	E	E _g	423	$\delta(\text{O}-\text{Si}-\text{O})$
	392		405, 389	A ₁ , E	T _{1u}		$\delta(\text{O}-\text{Si}-\text{O})$
			-, 340	A ₂ , E	T _{1g}	352	$\delta(\text{O}-\text{Si}-\text{O})$
329	333	315	314	A ₁	A _{2u}		$\delta(\text{O}-\text{Si}-\text{O})$
147, 173	143, 172/169	187, 171	173, 173	A ₁ , E	T _{2g}	171	$\delta(\text{O}-\text{Si}-\text{O})$
190/187	165/157	156/140	142	E	E _u		$\delta(\text{O}-\text{Si}-\text{O})$
	112/97	92		E	E _g	84	$\delta(\text{Si}-\text{O}-\text{Si})$

Ring-Opening Vibrations (400–500 cm⁻¹). The IR spectra of all monosubstituted compounds as well as of H₈Si₈O₁₂ show a broad absorption at ca. 470 cm⁻¹ and a sharp one at ca. 400 cm⁻¹ due to ring-opening vibrations. The Raman spectra are dominated by the strong peak at ca. 450 cm⁻¹, which is also due to a ring-opening vibration. This region will be treated more thoroughly in the next section.

Vibrations of the Framework below 400 cm⁻¹. Below 400 cm⁻¹ only Raman data are available. All monosubstituted compounds show a sharp line between 310 and 340 cm⁻¹, which is strongest for [Co(CO)₄(H₇Si₈O₁₂)] followed by PhH₇Si₈O₁₂. The intensity of this vibration correlates with the contribution of the Si–R stretching coordinate, which is considerable in [Co(CO)₄(H₇Si₈O₁₂)] (14%) and in Ph₇Si₈O₁₂ (8%) and can be neglected in (PhCH=CH)H₇Si₈O₁₂ and (PhCH₂CH₂)H₇Si₈O₁₂. This region is only in (PhCH₂CH₂)H₇Si₈O₁₂ in accordance with C_{3v} symmetry, all other spectra show additional features.

Ring-Opening Vibrations

The analysis of PhH₇Si₈O₁₂ and PhH₉Si₁₀O₁₅ has shown that the notion of ring-opening vibrations is also appropriate in the case of monosubstituted compounds. Ring-opening vibrations are defined as normal modes in which all Si–O stretching and/

SCHEME 2: Sets of Equivalent Rings of the Siloxane Cage $\text{RH}_7\text{Si}_8\text{O}_{12}$ ^a

^a The substituent is treated as a point mass.

or O–Si–O angle bending displacements of the considered ring are in phase.¹⁵ For octasilasesquioxanes a symmetry reduction from O_h to C_{3v} leads to two sets of equivalent coordinates for $\nu(\text{Si}-\text{O})$ and $\delta(\text{O}-\text{Si}-\text{O})$. Moreover, the cubes consist of two sets of equivalent rings as shown in Scheme 2.

The ring-opening vibrations of RH₇Si₈O₁₂ with R = Ph, CH=CHPh, CH₂CH₂Ph, and Co(CO)₄ were analyzed visually using the computer program MOBY⁴³ and correlated with the ring-opening vibrations of O_h-H₈Si₈O₁₂ (Table 7). This analysis revealed in two cases three and in two cases four A₁ and four E ring-opening vibrations for the monosubstituted compounds.

TABLE 7: Correlation of the Ring-Opening Vibrations of $\text{RH}_7\text{Si}_8\text{O}_{12}$ and $\text{H}_8\text{Si}_8\text{O}_{12}$

$\text{H}_8\text{Si}_8\text{O}_{12}$ calc	$\text{RH}_7\text{Si}_8\text{O}_{12}$											
	R = Ph			R = CH=CHPh			R = CH ₂ CH ₂ Ph			R = Co(CO) ₄		
	IR	Raman	calc	IR	Raman	calc	IR	Raman	calc	IR	Raman	calc
A_1	T_{1u} (481, rov)	475		478	469		477	468		486	469	480
	A_{1g} (446, rov)		462	467		455	446		452	444	461	468
	T_{2g} (418)		427	430							449	445
E	T_{1u} (397, rov)	401		403	402		402	395		393	399	402
	T_{1u} (481, rov)	475		500/491	469		492	468		492/490	469	487
	T_{2g} (418)		427	428/425		427	429/428		423	430/429		426
	E_g (423, rov)		412	422		411	422		410	422		422
	T_{1u} (397, rov)	401		399	388		399	402		399	399	398

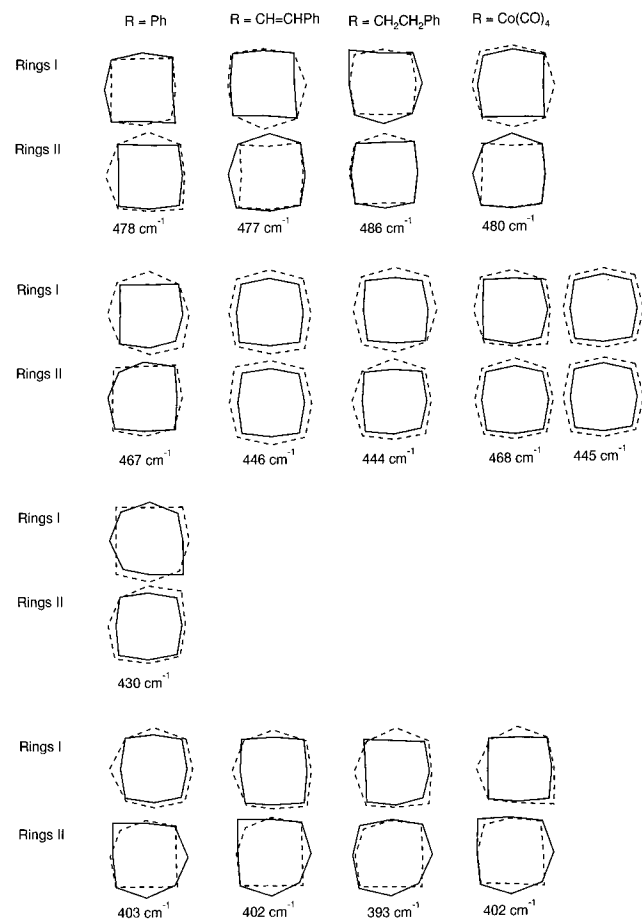


Figure 7. Visual representation of the A_1 ring-opening vibrations of the investigated $\text{RH}_7\text{Si}_8\text{O}_{12}$ compounds. The minimal and maximal displacements of the rings I and II, as defined in Scheme 2, are shown. The vibrations correlate from top to bottom with the $T_{1u} \nu_s(\text{Si}-\text{O}-\text{Si})$ (calc 481 cm^{-1}), the $A_{1g} \nu_s(\text{Si}-\text{O}-\text{Si})$ (446 cm^{-1}), the $T_{2g} \delta(\text{O}-\text{Si}-\text{O})$ (418 cm^{-1}), and the $T_{1u} \delta(\text{O}-\text{Si}-\text{O})$ (397 cm^{-1}) of $\text{H}_8\text{Si}_8\text{O}_{12}$.

The A_1 ring-opening vibrations are illustrated graphically in Figure 7. For each vibration the minimal and maximal displacements of the rings I and II are shown. In this representation the substituent is connected to the rings I at the down right position. As an effect of the symmetry reduction, the contribution of the $\nu(\text{Si}-\text{O})$ and/or $\delta(\text{O}-\text{Si}-\text{O})$ coordinates within one ring are different for some ring-opening vibrations, and in the case of $\text{PhH}_7\text{Si}_8\text{O}_{12}$, the ring-opening movement can be predominately located on either rings I or II. The A_1 mode, which correlates with the $T_{2g} \delta(\text{O}-\text{Si}-\text{O})$ at 418 cm^{-1} of $\text{H}_8\text{Si}_8\text{O}_{12}$, performs only in $\text{PhH}_7\text{Si}_8\text{O}_{12}$ a ring-opening movement and is therefore illustrated only for this molecule. In $[\text{Co}(\text{CO})_4(\text{H}_7\text{Si}_8\text{O}_{12})]$ two vibrations correlate with the totally symmetric

TABLE 8: Si-C Stretching Frequencies, Bond Distances, and Force Constants for Different Monosubstituted Octasilasesquioxanes

bond type	IR/ cm^{-1}	Raman/ cm^{-1}	calc/ cm^{-1}	% contribution of Si-C coordinate	$F(\nu(\text{SiC}))$ / $\text{mdyn}/\text{\AA}$	substituent
Si-C _{alkyl}	785 790	784	782	39	3.03	PhCH ₂ CH ₂ C ₆ H ₁₃
Si-C _{vinyl}	821	821	817	49	3.36	PhCH=CH
Si-C _{phenyl}	730	730	731	30	3.39	Ph
Si-C _{acetyl}					3.67 ^a	PhC≡C

^a Extrapolated.

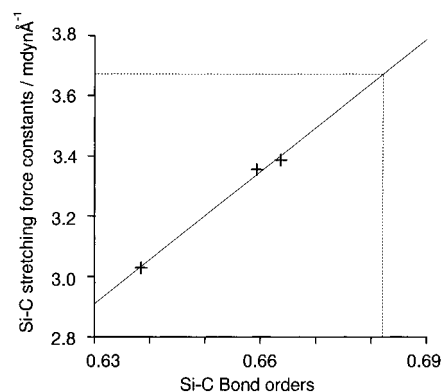
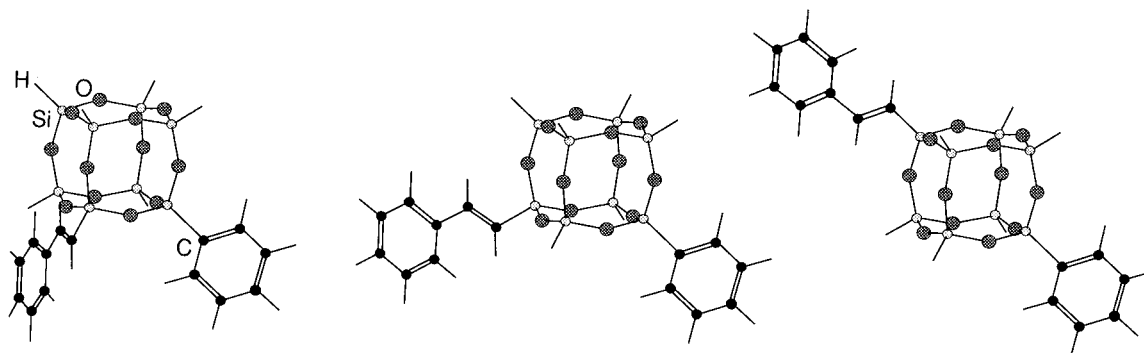


Figure 8. Dependence of the Si-C stretching force constants on the Si-C bond order. The crosses indicate the values for $(\text{PhCH}_2\text{CH}_2)\text{H}_7\text{Si}_8\text{O}_{12}$, $(\text{PhCH}=\text{CH})\text{H}_7\text{Si}_8\text{O}_{12}$, and $\text{PhH}_7\text{Si}_8\text{O}_{12}$. Extrapolation for $(\text{PhC}\equiv\text{C})\text{H}_7\text{Si}_8\text{O}_{12}$ leads to a Si-C stretching force constant of 3.67 $\text{mdyn}/\text{\AA}$.

ring-opening vibration calculated at 446 cm^{-1} in $\text{H}_8\text{Si}_8\text{O}_{12}$, which are both shown in Figure 7.

A strong dependence on the specific substituent exhibits the totally symmetric ring-opening vibration, which forms a very strong sharp peak at 456 cm^{-1} in the Raman spectrum of $\text{H}_8\text{Si}_8\text{O}_{12}$ (calculated at 446 cm^{-1}). This peak is the strongest feature in the Raman spectra of $(\text{PhCH}=\text{CH})\text{H}_7\text{Si}_8\text{O}_{12}$ and $(\text{PhCH}_2\text{CH}_2)\text{H}_7\text{Si}_8\text{O}_{12}$ and appears at 455 and 452 cm^{-1} , respectively. In $\text{PhH}_7\text{Si}_8\text{O}_{12}$ it is shifted to 462 cm^{-1} , and its intensity is reduced compared with that of $\text{H}_8\text{Si}_8\text{O}_{12}$. In $[\text{Co}(\text{CO})_4(\text{H}_7\text{Si}_8\text{O}_{12})]$ two rather strong peaks appear in this region at 461 and 449 cm^{-1} .

The different intensity of this vibration depending on the specific substituent can be qualitatively explained by investigating the potential energy distributions. In $\text{H}_8\text{Si}_8\text{O}_{12}$ as well as in $\text{RH}_7\text{Si}_8\text{O}_{12}$ (R = CH=CHPh and CH₂CH₂Ph) the Si-O stretching coordinate is mainly responsible for this vibration. Figure 7 shows that it performs a strong ring-opening movement of all six 4-rings. In $\text{PhH}_7\text{Si}_8\text{O}_{12}$ the vibrations at 427 and 462 cm^{-1} both perform a ring-opening movement, the ring-opening

SCHEME 3: Three Isomers of $\text{Ph}(\text{PhCH}=\text{CH})\text{H}_6\text{Si}_8\text{O}_{12}$ 

character of the one at 427 cm^{-1} being due to vibrational coupling with the mode at 462 cm^{-1} . This coupling is confirmed by the PED analysis, which shows a lower contribution of the Si–O stretching coordinate for the vibration at 462 cm^{-1} and a higher for the one at 427 cm^{-1} compared with the case of $\text{H}_8\text{Si}_8\text{O}_{12}$. This also leads to the decreased intensity of the mode at 462 cm^{-1} and the increased intensity of the one at 427 cm^{-1} as observed in the Raman spectrum (Figure 4). In $[\text{Co}(\text{CO})_4(\text{H}_7\text{Si}_8\text{O}_{12})]$ the PED analysis indicates considerable contributions of the Si–O stretching and the axial CoC stretching coordinates to the vibrations calculated at 468 and 445 cm^{-1} . Both correlate with the totally symmetric ring-opening vibration of $\text{H}_8\text{Si}_8\text{O}_{12}$ at 446 cm^{-1} , forming an in-phase and an out-of-phase combination with $\nu(\text{CoC})_{\text{ax}}$.

The E ring-opening vibrations of the monosubstituted compounds show a less pronounced dependence on the specific substituents than the A_1 modes. In Table 7 it can be seen that one E mode correlates with the T_{2g} mode of $\text{H}_8\text{Si}_8\text{O}_{12}$, which shows no ring-opening character. For $[\text{Co}(\text{CO})_4(\text{H}_7\text{Si}_8\text{O}_{12})]$ the two vibrations calculated at 426 and 422 cm^{-1} could not be observed in the Raman spectrum as they are covered by the strong $\nu(\text{CoC})_{\text{eq}}$ peak at 420 cm^{-1} .

Correlation of the Si–C Stretching Force Constants and Bond Orders

The compounds $\text{RH}_7\text{Si}_8\text{O}_{12}$ ($\text{R} = \text{CH}_2\text{CH}_2\text{Ph}$, $\text{CH}=\text{CHPh}$, and Ph) exemplify Si– C_{alkyl} , Si– C_{vinyl} , and Si– C_{phenyl} bonds, respectively. The corresponding stretching frequencies and force constants are listed in Table 8. The potential energy distribution indicates contributions of the Si–C stretching coordinate between 30 and 50%. As different coordinates participate in these vibrations, the frequency positions will be influenced by contributions from several coordinates, and it is therefore not possible to deduce a trend for the Si–C bond orders on the basis of the measured frequencies. In the case of $\text{PhH}_7\text{Si}_8\text{O}_{12}$ also a mass effect could be responsible for the low Si–C stretching frequency, the higher mass in this case being due to the direct connection of the phenyl ring to the siloxane cage. More representative for the bond strengths than the frequencies are the force constants. Table 8 shows that the force constants indicate indeed a different trend than the frequencies with a stronger Si–C bond for Si– C_{phenyl} and Si– C_{vinyl} than Si– C_{alkyl} . It seemed therefore interesting to compare the force constant trend with the Si–C bond orders of $\text{RH}_7\text{Si}_8\text{O}_{12}$ ($\text{R} = \text{CH}_2\text{CH}_2\text{Ph}$, $\text{CH}=\text{CHPh}$, and Ph) calculated by the EHMO method.⁴⁴ For this calculation the same parameters were used as in ref 45. Figure 8 shows that the force constants and the bond orders both increase in the series Si– C_{alkyl} , Si– C_{vinyl} , Si– C_{phenyl} . The extrapolation for $(\text{PhC}\equiv\text{C})\text{H}_7\text{Si}_8\text{O}_{12}$ leads to a force constant value $F(\nu(\text{SiC}_{\text{acetyl}})) = 3.67\text{ mdyne/\AA}$.

Conclusions

The IR and Raman spectra of the monosubstituted hydrosilasesquioxanes $\text{RH}_7\text{Si}_8\text{O}_{12}$ ($\text{R} = \text{Co}(\text{CO})_4$, Ph , $\text{CH}=\text{CHPh}$, and $\text{CH}_2\text{CH}_2\text{Ph}$) have been analyzed by spectral correlation and a normal coordinate analysis. Special attention was paid to the Si–C stretching and the ring-opening vibrations. Although most spectral features of the siloxane cages could be understood assuming a local C_{3v} symmetry, vibrations indicating a lower symmetry occurred in all monosubstituted compounds and were due to vibrational coupling with modes of the substituent. Especially the totally symmetric ring-opening vibration at 456 cm^{-1} in the Raman spectrum of $\text{H}_8\text{Si}_8\text{O}_{12}$ showed a specific dependence on the different substituents. The molecules $\text{PhH}_7\text{Si}_8\text{O}_{12}$, $(\text{PhCH}=\text{CH})\text{H}_7\text{Si}_8\text{O}_{12}$, and $(\text{PhCH}_2\text{CH}_2)\text{H}_7\text{Si}_8\text{O}_{12}$ have allowed the investigation of the organic-substituted siloxane cage $\text{CH}_7\text{Si}_8\text{O}_{12}$, contributing each a case of an Si– C_{phenyl} , Si– C_{vinyl} , and Si– C_{alkyl} bond, respectively. To complete this series, an Si–C stretching force constant was extrapolated for $(\text{PhC}\equiv\text{C})\text{H}_7\text{Si}_8\text{O}_{12}$. The silasesquioxane $[\text{Co}(\text{CO})_4(\text{H}_7\text{Si}_8\text{O}_{12})]$, which exhibits a silicon–metal bond, could be analyzed the same way as the organic-substituted compounds and showed a similar pattern for the siloxane cage vibrations.

This analysis forms the basis for the investigation of the siloxane cage vibrations occurring in disubstituted octahydrosilasesquioxanes $\text{R}'\text{R}''\text{H}_6\text{Si}_8\text{O}_{12}$ and for the study of the vibrational interactions between the two substituents R' and R'' in these systems. Three isomers exist in the case of disubstitution as shown in Scheme 3 for $\text{R}' = \text{Ph}$ and $\text{R}'' = \text{CH}=\text{CHPh}$. These compounds should become available by hydrosilylation of a monosubstituted hydrosilasesquioxane and subsequent separation of the mixtures.⁴⁶

Acknowledgment. This work was supported by the Schweizerischer Nationalfonds zur Förderung der wissenschaftlichen Forschung (Project NF 20-46617.96).

References and Notes

- Voronkov, M. G.; Lavrent'yev, V. I. *Top. Curr. Chem.* **1982**, *102*, 199.
- Mehl, G. H.; Goodby, J. W. *Angew. Chem.* **1996**, *108*, 2791.
- Bassindale, A. R.; Gentle, T. E. *J. Mater. Chem.* **1993**, *3*, 1319.
- Hoebbel, D.; Pitsch, I.; Heidemann, D. *Z. Anorg. Allg. Chem.* **1991**, *592*, 207.
- Haddad, T. S.; Lichtenhan, J. D. *J. Inorg. Organomet. Polym.* **1995**, *5*, 237.
- Agaskar, P. A. *J. Am. Chem. Soc.* **1989**, *111*, 6858.
- Agaskar, P. A. *Inorg. Chem.* **1990**, *29*, 1603.
- Yuchs, S. E.; Carrado, K. A. *Inorg. Chem.* **1996**, *35*, 261.
- Harrison, P. G.; Kannengiesser, R. *J. Chem. Soc., Chem. Commun.* **1995**, 2065.
- Sellinger, A.; Laine, R. M. *Chem. Mater.* **1996**, *8*, 1592.
- Sellinger, A.; Laine, R. M. *Macromolecules* **1996**, *29*, 2327.
- Sasamori, R.; Okau, Y.; Isobe, T.; Matsuda, Y. *Science* **1994**, *265*, 1691.

- (13) Bieniok, A. M.; Bürgi, H.-B. *J. Phys. Chem.* **1994**, *98*, 10735.
- (14) Bärtsch, M.; Bornhauser, P.; Calzaferri, G.; Imhof, R. *J. Phys. Chem.* **1994**, *98*, 2817.
- (15) Bornhauser, P.; Calzaferri, G. *J. Phys. Chem.* **1996**, *100*, 2035.
- (16) de Man, A. J. M.; Sauer, J. *J. Phys. Chem.* **1996**, *100*, 5025.
- (17) Tossell, J. A. *J. Phys. Chem.* **1996**, *100*, 14828.
- (18) Pasquarello, A.; Hybertsen, M. S.; Car, R. *Phys. Rev.* **1996**, *B54*, R2339.
- (19) Auf der Heyde, T. P. E.; Bürgi, H.-B.; Bürgy, H.; Törnroos, K. W. *Chimia* **1991**, *45*, 38.
- (20) Törnroos, K. W. *Acta Crystallogr.* **1994**, *C50*, 1646.
- (21) Kowalewski, J.; Nilsson, T.; Törnroos, K. W. *J. Chem. Soc., Dalton Trans.* **1996**, 1597.
- (22) Marcolli, C.; Lainé, P.; Bühler, R.; Calzaferri, G.; Tomkinson, J. *J. Phys. Chem. B* **1997**, *101*, 1171.
- (23) Calzaferri, G.; Herren, D.; Imhof, R. *Helv. Chim. Acta* **1991**, *74*, 1278.
- (24) Hendan, B. J.; Marsmann, H. C. *J. Organomet. Chem.* **1994**, *483*, 33.
- (25) Dittmar, U.; Hendan, B. J.; Flörke, U.; Marsmann, H. C. *J. Organomet. Chem.* **1995**, *489*, 185.
- (26) Bürgy, H.; Calzaferri, G. *J. Chromatogr.* **1990**, *507*, 481.
- (27) Calzaferri, G.; Imhof, R.; Törnroos, K. W. *J. Chem. Soc., Dalton Trans.* **1993**, 3741.
- (28) Calzaferri, G.; Imhof, R.; Törnroos, K. W. *J. Chem. Soc., Dalton Trans.* **1994**, 3123.
- (29) Calzaferri, G.; Marcolli, C.; Imhof, R.; Törnroos, K. W. *J. Chem. Soc., Dalton Trans.* **1996**, 3313.
- (30) Marcolli, C.; Imhof, R.; Calzaferri, G. *Microchim. Acta* **1997** (Suppl. 14), 493.
- (31) Wilson, E. B., Jr.; Decius, J. C.; Cross, P. C. *Molecular Vibrations*; McGraw-Hill Book Co.: New York, 1955.
- (32) McIntosh, D. F.; Peterson, M. R. *General Vibrational Analysis System*; QCPE Program No. QCMP067, 1988.
- (33) van den Berg, G. C.; Oskam, A. *J. Organomet. Chem.* **1974**, *78*, 357.
- (34) Marcolli, C. Ph.D. Thesis, Universität Bern, 1996.
- (35) Calzaferri, G.; Brändle, M. QCMP No. 116. *QCPE Bull.* **1992**, *12* (4) (update May 1993).
- (36) Calzaferri, G.; Rytz, R. *J. Phys. Chem.* **1996**, *100*, 11122.
- (37) van den Berg, G. C.; Oskam, A.; Vrieze, K. *J. Organomet. Chem.* **1973**, *57*, 329.
- (38) van den Berg, G. C.; Oskam, A. *J. Organomet. Chem.* **1975**, *91*, 1.
- (39) Darensbourg, D. J.; Brown, T. L. *Inorg. Chem.* **1968**, *7*, 959.
- (40) Brown, T. L.; Darensbourg, D. J. *Inorg. Chem.* **1967**, *6*, 971.
- (41) Darensbourg, D. J. *Inorg. Chim. Acta* **1970**, *4*, 597.
- (42) Bor, G. *Inorg. Chim. Acta* **1967**, *1*, 81.
- (43) Höweler, U. *MOBY*, Molecular Modelling on the PC, Version 1.6F; Springer-Verlag: Berlin, 1993.
- (44) Hoffmann, R. *J. Chem. Phys.* **1963**, *39*, 1397.
- (45) Bärtsch, M.; Calzaferri, G.; Marcolli, C. *Res. Chem. Intermed.* **1995**, *21*, 577.
- (46) Aebi, B.; Calzaferri, G.; Herren, D.; Imhof, R.; Schlunegger, U. P. *Rapid Commun. Mass Spectrom.* **1996**, *10*, 1607.